Long-wavelength adaptation reveals slow, spectrally opponent inputs to the human luminance pathway

Andrew Stockman

Institute of Ophthalmology, University College London,
London, UK

Daniel J. Plummer

Department of Psychology, University of California San Diego,
La Jolla, CA, USA

In addition to its expected fast, additive L- and M-cone inputs (L + M), the luminance pathway has slow, spectrally opponent inputs. We have previously shown that on long-wavelength fields, the dominant slow signals change from L–M at moderate intensity levels to M–L signals at high. Here, we focus on the transition between them, which we find is marked by substantial changes in temporal phase delay, and by large and unexpected shifts in flicker spectral sensitivity. At moderate temporal frequencies, counter to the selective adaptation caused by the field, spectral sensitivity changes from being M-cone-like to more L-cone-like. These changes can be accounted for by a change in the relative strengths of the slow spectrally opponent cone signals from L–M exceeding M–L below the transition to M–L exceeding L–M above it, and by the resulting changes in constructive and destructive interference between the dominant signal components. We speculate that the transition is caused by the deep-red field becoming equivalent, postreceptorally, to a green field at high bleaching levels. These results further challenge the dogma that there are separable psychophysical channels for the transmission and processing of color and luminance information. Although its output generates an achromatic percept, the luminance channel has spectrally opponent inputs.

Keywords: Color vision, Postreceptoral channels, Flicker sensitivity, Phase differences, Luminance, Chromatic

Introduction

According to the conventional model of the human visual system, signals from the three cones [short (S)-, middle (M)-, and long (L)-wavelength-sensitive] feed either into the additive, fast luminance channel (L + M), or into the more sluggish spectrally opponent chromatic channels (L − M) or (S − [L + M]) (e.g., Boynton, 1979; De Lange, 1958b; Eisner & MacLeod, 1980; Guth, Alexander, Chumbly, Gillman, & Patterson, 1968; Luther, 1927; Schrödinger, 1925; Smith & Pokorny, 1975; Walls, 1955). In two recent papers, we have documented several failures of this conventional model and have developed a new model that can account for them (Stockman & Plummer, 2005; Stockman, Plummer, & Montag, 2005). The most serious failures are the large phase adjustments often required to produce flicker nulls (see also Cushman & Levinson, 1983; De Lange, 1958b; Lindsey, Pokorny, & Smith, 1986; Smith, Lee, Pokorny, Martin, & Valberg, 1992; Swanson, Pokorny, & Smith, 1987; Walraven & Leebeek, 1964), which are typically accompanied by substantial frequency-dependent changes in flicker detection spectral sensitivity and modulation sensitivity. These failures, which are too large to be accounted for by the addition of fast M- and L-cone signals of the same sign, demonstrate that the perception of achromatic flicker depends on slow spectrally opponent signals as well as fast additive ones (Stockman & Plummer, 2005; Stockman

et al., 2005). Examples of the large phase adjustments can be seen in Figures 1 and 3, whereas examples of the frequency-dependent changes in spectral sensitivity can be seen in Figure 4.

The idea of simple, separable psychophysical pathways for the transmission and processing of color and luminance information is also under scrutiny because of growing physiological and anatomical evidence for the mixing of parvocellular and magnocellular signals at the retina and cortex (see Discussion section). Our psychophysical results show that this mixing may have perceptual significance.

The interactions between the additive and spectrally opponent cone signals are most readily revealed in phase data. Our previous M- and L-cone phase data are summarized in Figure 1 for subject AS (left panels) and subject DP (right panels) at four levels of a 658-nm background: 8.93 (Level 1), 10.16 (Level 2), 11.18 (Level 3), and 12.50 (Level 4) $\log_{10}$ quanta s^{-1} deg^{-2}. Subjects were presented with sinusoidally flickering target stimuli superimposed in the center of the 658-nm background under conditions that eliminated S-cone and rod responses. The targets were 4° of visual angle in diameter, and the background 9°. Fixation was central. Phase measurements were made either between an M-cone flickering stimulus (a pair of alternating lights equated for the L-cones, so that their alternation was visible only to the M-cones) and a 656-nm flickering stimulus, or between an L-cone flickering stimulus (a pair of alternating lights equated for the M-cones) and a 656-nm flickering stimulus. Flicker
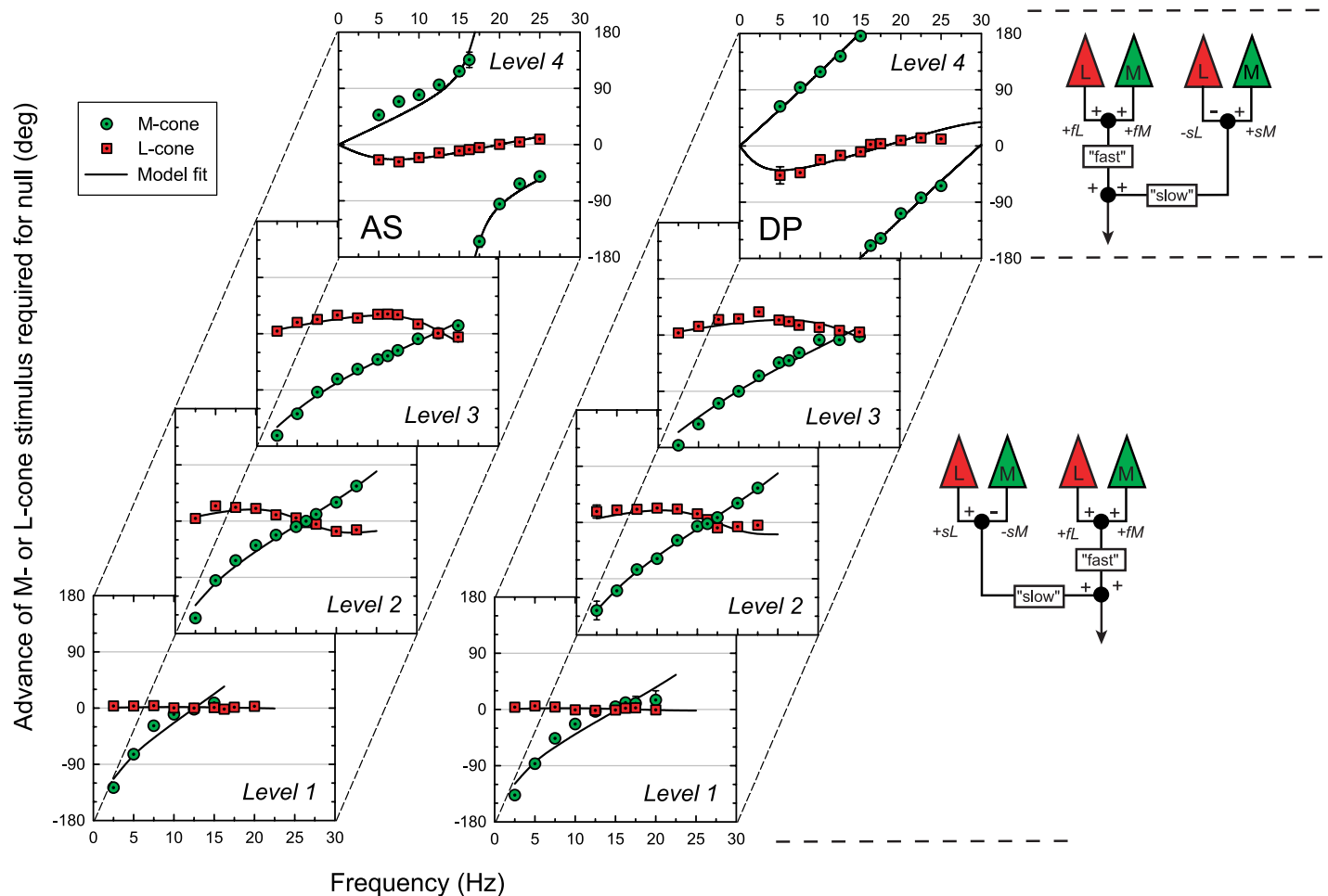
Figure 1. Phase advances of M-cone (green dotted circles) or L-cone (red dotted squares) stimuli required to null a 656-nm target measured on 658-nm backgrounds of 8.93 (Level 1), 10.16 (Level 2), 11.18 (Level 3), or 12.50 (Level 4) $\log_{10}$ quanta s^{-1} deg^{-2}. The M-cone stimuli were alternating pairs of L-cone-equated 540 and 650 nm targets; and the L-cone stimuli were pairs of M-cone-equated 650 and 550 nm targets. The continuous lines are fits of a model in which the cone signals are assumed to be the resultant of a fast signal and a delayed slow signal of the same or opposite sign. Left panels: AS. Right panels: DP. For further details, see Stockman et al. (2005) and Stockman & Plummer (2005). At Levels 1, 2, and 3, the dominant cone signals underlying the phase data are assumed to be +fM+fL and −sM+sL (lower right circuit), whereas at Level 4 they are assumed to be +fM+fL and +sM−sL (upper right circuit).

frequencies of between 2.5 and 25 Hz were used. Initially, the flickering stimuli were alternated, and the subjects were asked to adjust their relative phase (and amplitude) to null or cancel the perception of flicker. The data in Figure 1 show the phase adjustments away from opposite phase that are required to null either M-cone flicker (green dotted circles) or L-cone flicker (red dotted squares) with the 656-nm flicker (i.e., flicker "equichromatic" with the background, and which is thus unlikely to generate a substantial spectrally opponent or chromatic flicker signal; see also below). Zero degree on these plots means that the two lights cancelled when they were physically in opposite phase (i.e., when they were alternated), whereas ±180° means that they cancelled when they were in the same phase. Thus, the plotted phase delays indicate those delays introduced within the visual system. As can be seen, some of the phase adjustments are substantial even at moderately high temporal frequencies. They are inconsistent

with the conventional model of luminance, which, apart from phase differences that arise because of the selective adaptation of the L-cones by the long-wavelength field, predicts that no phase adjustments should be required.

The data shown in Figure 1 illustrate another intriguing effect. In our previous papers, we emphasized that some of the phase adjustments are large, particularly for the nulls involving M-cone flicker. What we did not emphasize is the abrupt change in the signs of the M- and L-cone phase delays that occurs between two critical level (Levels 3 and 4). That change is the focus of the measurements and analysis presented in this paper.

Working model

For the interpretation of our data, we assume that the channel that underlies the perception of achromatic flicker
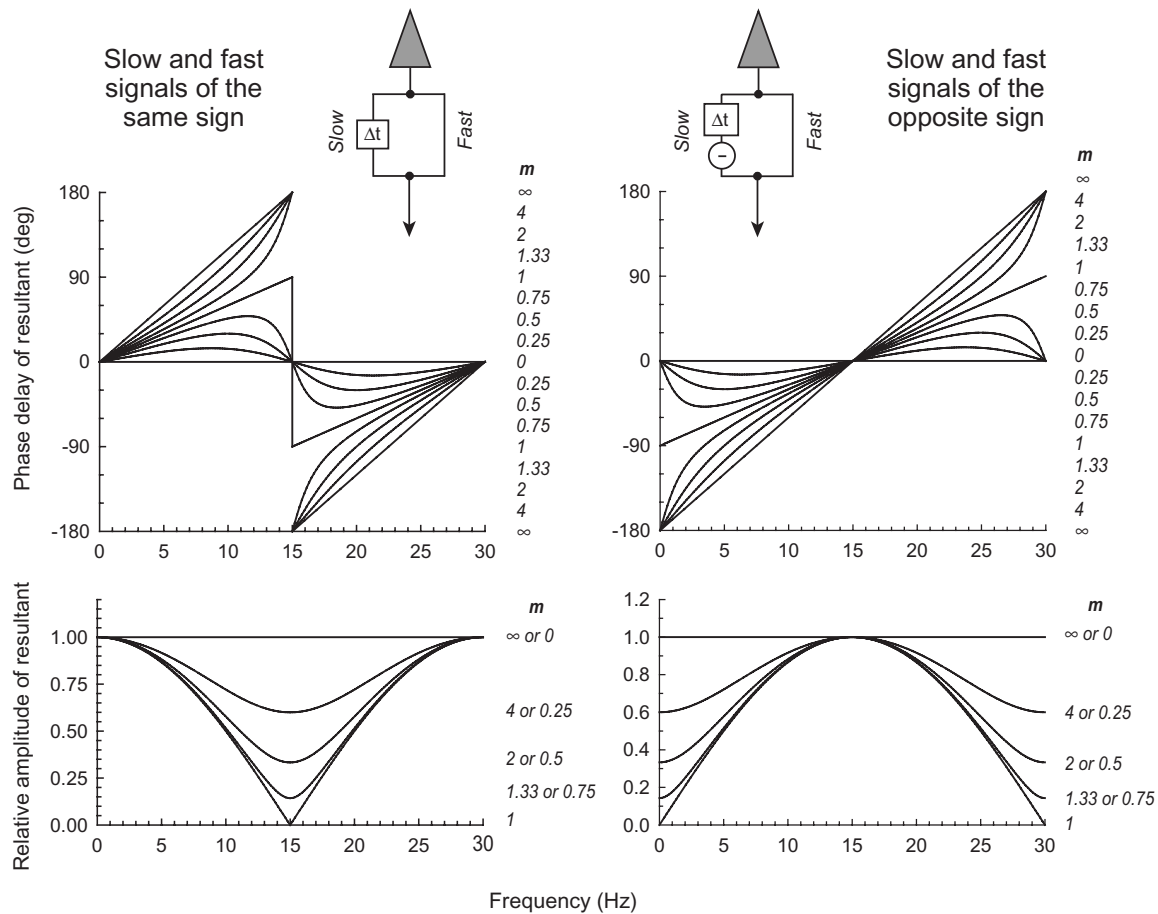
Figure 2. Model predictions of the phase delay (upper panels) and relative amplitude (lower panels) of the resultant of the combination of slow and fast signals of the same sign (left panels) and of opposite sign (right panels). Predictions are shown for slow to fast signal ratios, *m*, ranging from 0 to ∞, and for a time delay, Δ*t*, between the slow and fast signals of 33.33 ms.

generates a univariant flicker signal, although its several input signals can be substantially delayed relative to each other and can be of either positive or negative sign. Thus, two flickering lights of any wavelength composition detected solely by that channel can be flicker-photometrically cancelled or nulled by adjusting their relative amplitude and phase. Under the conditions of our experiments, we find that nulls are generally possible near-flicker-threshold at all frequencies above c. 5 Hz. Flicker nulls can also be set at 2.5 Hz under most conditions. In our previous work, we found evidence for multiple cone inputs to the achromatic flicker channel, which we refer to as "M" or "L", according to the cone type from which the input signals originate, prefixed by "f" or "s" for fast or slow, and by "+" or "−" according to their polarity with respect to the fast signals. For a given condition, the resultant signal from a particular cone type is assumed to be the vector sum of its slow and fast signal components, which have some fixed ratio of signal amplitudes (*m*) and are separated by a delay of Δ*t* (ms). Importantly, the slow cone signal can be of the same or opposite sign as the fast cone signal. Some examples of the model pre-

dictions are shown in Figure 2 for slow and fast signals of the same polarity (left panels) or of the opposite polarity (right panels). The horizontal and diagonal lines in the upper panels, respectively, represent the phase delays of the fast signal alone (*m* = 0) and the slow signal alone (*m* = ∞) signals. The relative delay of the slow signal (Δ*t*) in these examples is 33.3 ms, as a result of which slow and fast signals of the same polarity become opposite in phase at 15 Hz and destructively interfere (left panel), whereas slow and fast of the opposite polarity become the same in phase at 15 Hz and constructively interfere (right panel). Predictions are shown in Figure 2 for several values of *m*.

The upper panels show the predicted phase delay of the combined slow and fast signals, and the lower panels show their amplitudes. The phase delays are related to the phase adjustments required to null flickering lights (Figures 1 and 3), whereas the amplitudes are related to the flicker detection sensitivities (Figures 4 and 5). The amplitude predictions illustrate the effects of destructive and constructive interference and its dependence on flicker frequency. The phase predictions are characteristic

Subject	Level	M			L		
		Slow/fast (*m*)	Δt	Slow sign	Slow/fast (*m*)	Δt	Slow sign
AS	1	1.79	39.82	Minus	0.03	25.22	Plus
	2	2.44	31.48	Minus	0.32	31.63	Plus
	3	2.87	22.72	Minus	0.49	21.60	Plus
	4	1.31	29.50	Plus	0.40	25.08	Minus
DP	1	1.67	32.70	Minus	0.04	29.94	Plus
	2	3.15	30.74	Minus	0.33	28.81	Plus
	3	4.51	21.71	Minus	0.41	20.57	Plus
	4	27.96	33.56	Plus	0.63	27.79	Minus

Table 1. Parameters of time delay model fitted to M- and L-cone phase data shown in Figure 1. The parameters are the ratio of slow/fast signal size, the time delay (Δt) in ms between the slow and fast signals, and the sign of the slow signal with respect to that of the fast. For details see text.

"signatures" that should be found in any experimental data that reflect the simple combination of slow and fast signals. A comparison between the phase signatures and the phase data of Figure 1 shows that the two are indeed similar, which suggests the phase data are broadly consistent with our model. The continuous lines in Figure 1 are fits of this model to the M- and L-cone phase data. At Levels 1–3 (8.93–11.18 $\log_{10}$ quanta s^{-1} deg^{-2}), the dominant slow and fast signals are +sL, −sM, +fL, and +fM, as illustrated in the lower right circuit diagram of Figure 1, whereas at Level 4 (12.50 $\log_{10}$ quanta s^{-1} deg^{-2}) they are −sL, +sM, +fL, and +fM, as illustrated in the upper right circuit diagram. Table 1 summarizes the best-fitting model parameters for the fits to the M- and L-cone data shown in Figure 1. The slow/fast signal ratios (*m*) are typically small for L-cone signals and large for M-cone signals, whereas Δt varies between 20 and 40 ms. (The values for Level 1 are anomalous, because the equichromatic target is below M-cone threshold and is therefore an L-cone stimulus.)

The crucial change in the model parameters that occurs between Levels 3 and 4 (11.18 and 12.50 log quanta s^{-1} deg^{-2}) is that the polarities of the both the slow M-cone and the slow L-cone signals reverse. Thus, the slow, spectrally opponent signals change from +sL−sM to −sL+sM. In this paper, we focus on the changes in phase delay and flicker spectral sensitivity that occur between Levels 3 and 4.

Methods

Apparatus

The optical apparatus was a conventional five-channel, Maxwellian-view optical system with a 2-mm entrance pupil illuminated by a 900-W Xenon arc. Wavelengths were selected by the use of interference filters with full-width at half-maximum bandwidths of between 7 and 11 nm (Ealing or Oriel). The radiance of each beam could be varied by the insertion of fixed neutral density filters (Oriel) or under computer control by the rotation of circular, variable neutral density filters (Rolyn Optics). Sinusoidal modulation was produced by the pulse-width modulation of fast, liquid crystal light shutters (Displaytech) at a carrier frequency of 400 Hz. The position of the observer's head was maintained by a dental wax impression. The apparatus is described in more detail elsewhere (Stockman et al., 2005).

Stimuli

In all experiments, target stimuli of 4° of visual angle in diameter were superimposed in the center of a steady 658-nm background field of 9° in diameter. Fixation was central. Calibrations were carried out with the use of a UDT Radiometer and a spectroradiometer (E,G & G). For further details, see Stockman et al. (2005).

Backgrounds

The 658-nm background was varied in radiance from 10.39 to 12.38 $\log_{10}$ quanta s^{-1} deg^{-2}. Given the relative insensitivity of rods and S-cones to the long-wavelength fields, it was important to ensure that the rods and S-cones did not detect the 520-nm target. To desensitize the rods and S-cones, an auxiliary 410-nm background of 10.30 $\log_{10}$ quanta s^{-1} deg^{-2} was superimposed on the 658-nm background. Given that the S-cones are one log unit more sensitive to the auxiliary background wavelength of 410 nm than they are to the shortest target wavelength of 520 nm (Stockman & Sharpe, 2000), the S-cone modulations produced by the 520-nm targets (see Figure 5 for the radiances used) were well below S-cone modulation threshold (see Stockman, MacLeod, & DePriest, 1991). As expected, therefore, in control experiments we could find no evidence that the S-cones contributed to our measurements.

We used single or combined 520 and 650 nm monochromatic targets. Flicker frequencies of 2.5, 7.5, 15, and 22.5 Hz were used. Monochromatic targets were used rather than cone-isolating targets, because of the large and abrupt changes in phase delay and spectral sensitivity that occur between Levels 3 and 4. M- and L-cone-isolating targets require the use of paired, alternating stimuli that are equated for (and therefore invisible to) the unwanted cone type. We were concerned that paired targets that were slightly imperfectly equated could generate small signals from the unwanted cone type. Although usually well below threshold, such signals could become visually significant if the resultant signals from the wanted cone type are cancelled by destructive interference, which is likely under some of the conditions of our experiment. Using monochromatic lights avoids this problem but means that the phase lags are harder to interpret because most spectral targets typically produce both M- and L-cone signals even on the 658-nm background (see below).

The 520-nm target

Although the flickering 520-nm target generates predominantly an M-cone signal on the long-wavelength background, it also generates a small L-cone signal (a shorter wavelength target would have reduced the L-cone contribution but would have had the unwanted effect of increasing the likelihood of an S-cone contribution). This small L-cone signal is evidenced by the slow/fast signal ratios (m) values for 500 and 540 nm flickering targets being less than the m values for pure M-cone targets (Stockman & Plummer, 2005; Stockman et al., 2005). The slow component of the L-cone signal produced by the 520-nm target is much smaller than the fast L-cone component (see Table 1) and is cancelled by the stronger opposite polarity slow M-cone signals. Consequently, the L-cone signal produced by the 520-nm target can be thought of as mainly a fast +fL signal, which adds to the fast M-cone signal (+fM).

For the interpretation of our data, therefore, we assume that the 520-nm flickering light generates −sM, +fM, and +fL flicker signals at lower 658 nm intensity levels and +sM, +fM, and +fL flicker signals at higher levels.

The 650-nm target

On the long-wavelength 658-nm background, the flickering 650-nm target generates both M- and L-cone flicker signals (once, that is, the target is intense enough to exceed M-cone flicker threshold, which is not the case at Level 1). Because the 650-nm target is approximately equichromatic with the 658-nm background, it produces mainly luminance modulation with comparatively little chromatic modulation. We assume, therefore, that it generates predominantly fast signals (+fL and +fM). This assumption implies that the two opposing slow signals are

roughly balanced under these conditions (i.e., −sM ≈ +sL and +sM ≈ −sL) and cancel; an assumption for which there is good evidence under a variety of conditions for conventional chromatic channels (Chaparro, Stromeyer, Chen, & Kronauer, 1995; Eskew, McLellan, & Giulianini, 1999; Stromeyer, Cole, & Kronauer, 1985). If, contrary to this assumption, the spectrally opponent signals are slightly unbalanced, and the equichromatic flickering target does generate a small slow signal, then the relative strengths of the slow signal will be underestimated for the 650-nm target and overestimated for the 520-nm target. For the interpretation of our data, we assume that the 650-nm flickering light generates +fM and +fL flicker signals.

The flickering targets were continuously presented, so that in the central 4° observers were adapted to the mean radiance of the flickering targets plus the steady background. The amplitude threshold radiances of the flickering targets are plotted in Figure 5 (their mean radiances are 0.3 log unit less than the plotted values). Under most conditions, the target radiances are small relative to the background radiance, so that the targets shift the effective adapting wavelength from the field wavelength of 658 nm to wavelengths only 4-nm shorter or usually less. The only conditions under which the 520-nm target is bright enough to cause sizeable wavelength shifts are at 15 and 22.5 Hz for DP at the very highest background radiances, where the loss of sensitivity to 520-nm flicker significantly exceeds Weber's Law (see Figure 5). The worst case is at 22.5 Hz at the highest background radiance, where the effective wavelength is shifted by 12nm to 646 nm. This slightly shifts the Weber predictions (see below) but does not affect the conclusions. The effective adapting wavelength was calculated by finding the wavelength that gives rise the same relative L- and M-cone excitation as the combined background and targets according to the Stockman and Sharpe (2000) cone fundamentals.

Procedures

Subjects light adapted to the target and background fields for at least 3 min prior to any data collection. During the experiment, each subject interacted with the computer by means of eight buttons on a keypad. The computer provided instructions and gave verbal and other auditory feedback by way of a voice synthesizer and tones.

Flicker thresholds were found by the method of adjustment. The modulation of the flickering stimulus was set to the maximum level of 92% and its amplitude was varied to find the threshold for detecting the flicker. Phase differences were measured between the superimposed 520 and 650 nm flickering lights using a flicker cancellation technique. First, each subject adjusted the modulation of the two lights separately (with the other light set at zero modulation) until the flicker was just above threshold (typically c. 0.2 $\log_{10}$ above threshold). Then, the subject adjusted the phase difference between the two lights and if nec-

essary their relative modulation to find the best flicker null. Subjects could also reverse the relative phase of the two stimuli by 180° to help them find the correct nulling phase.

Except where noted, all data points are averaged from three or four settings made on at least four separate runs. Other details of the experimental procedures are given in the Results section.

Subjects

The two observers in this work were the authors (AS and DP). Both observers were male, had normal color vision, and were emmetropic. These studies conform to the standards set by the Declaration of Helsinki, and the procedures have been approved by local ethics committees in the United Kingdom and United States.

Results

Phase delays

The phase delays of 520-nm flicker required to null the 650-nm equichromatic flicker are shown in Figure 3 for AS (top panel) and DP (bottom panel), measured as a function of the radiance of the 658-nm background. Flicker frequencies of 2.5 (circles), 7.5 (squares), 15 (triangles), and 22.5 (inverted triangles) Hz were used. Below 11.21 $\log_{10}$ quanta s^{-1} deg^{-2} (highlighted by the pink area) and above 12.13 $\log_{10}$ quanta s^{-1} deg^{-2} (highlighted by the green area), the phase delays are relatively constant. In between, there are substantial phase shifts.

The black symbols show the M-cone phase delays measured at the corresponding frequencies at Levels 3 and 4 replotted from Figure 1 (2.5 Hz phase delays could not be measured at the highest level). The phase differences below 11.21 $\log_{10}$ quanta s^{-1} deg^{-2} are similar to the M-cone phase delays measured at Level 3, whereas those above 12.13 $\log_{10}$ quanta s^{-1} deg^{-2} are similar to the M-cone phase delays measured at Level 4. In most cases, the 520-nm phase delays are slightly less than those for the M-cones. This difference arises because the 520-nm target generates a small L-cone signal, which is also found for 500 and 540 nm targets (see Stockman & Plummer, 2005; Stockman et al., 2005).

The abrupt changes in the phase delay in the unshaded area are largest at 2.5 Hz but then fall off as the frequency increases. They are close to 180° at 2.5 Hz for both AS and DP. For AS, they then fall to c. 130° at 7.5 and 15 Hz, and to 50° at 22.5 Hz. For DP, they remain large at 170° at 7.5 Hz and 200° at 15 Hz and then fall to 40° at 22.5 Hz. The differences between AS and DP are consistent with previous measurements that indicate that the slow M-cone signals for DP are stronger (relative to his fast M-cone
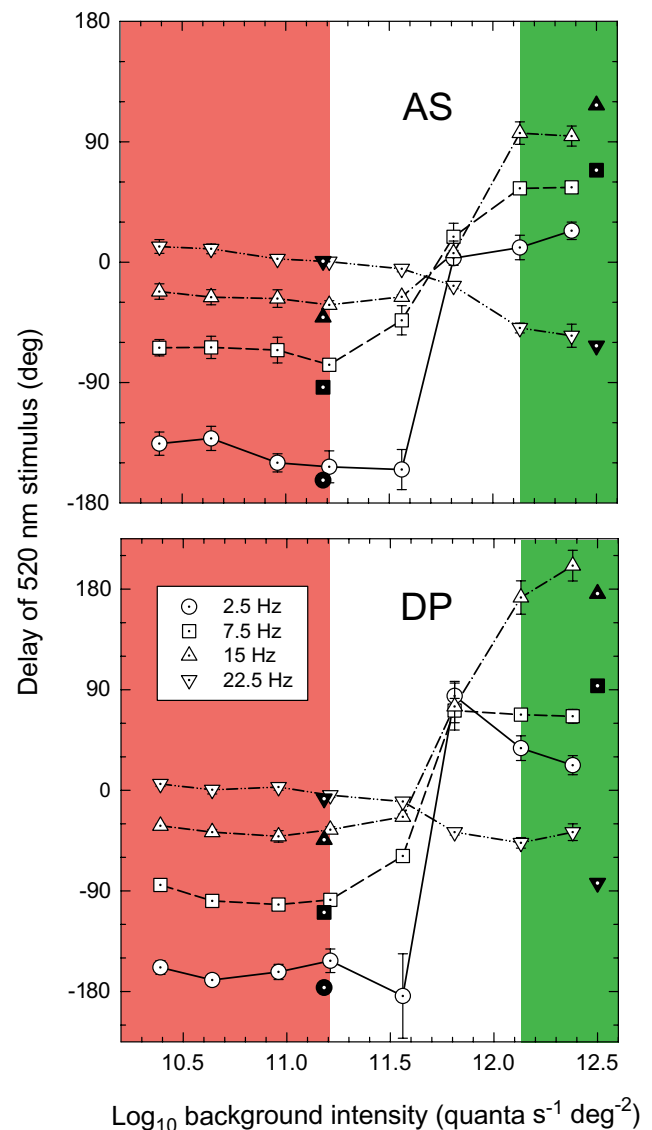

Figure 3. Phase advances of a 520-nm target required to null a 650-nm target measured as a function of the radiance of the 658-nm background. Data are shown for 2.5 (dotted white circles), 7.5 (dotted white squares), 15 (dotted white triangles), and 22.5 (dotted white inverted triangles) Hz flicker. The pink area (here and in Figures 4 and 5) indicates the lower radiance range within which the phase delays are consistent with the 520-nm flicker generating mainly a −sM signal, whereas the green area indicates the higher radiance range within which the phases are consistent with it generating mainly a slow +sM signal. The filled symbols are the corresponding M-cone phase delays from Figure 1 for 2.5 (dotted black circles), 7.5 (dotted black squares), 15 (dotted black triangles), and 22.5 (dotted white inverted triangles) Hz. Top panel: AS. Bottom panel: DP.

signals) than they are for AS (Stockman & Plummer, 2005; Stockman et al., 2005).

According to our model, the changes in phase delay between 520 and 650 nm flicker should reflect the

transition from the 520-nm flicker generating predominantly $-sM+fM(+fL)$ signals at low levels to it generating predominantly $+sM+fM(+fL)$ signals at high levels. Our data are broadly consistent with such a reversal of the slow M-cone signal because the phase adjustments change by c. 180° at low to moderate frequencies. At 22.5 Hz, however, the change is only 40° or 50°. There are two likely reasons for the shortfall at this frequency. First, the slow $+sM-sL$ signals above the transition are slower than the $-sM+sL$ signals below it (compare the phase delay slopes in Figure 1 and the Δt estimates in Table 1 for Levels 3 and 4). As a result, the two opposing pairs of slow signals ($-sM+sL$ versus $+sM-sL$) are only about 90–120° apart at 22.5 Hz. Second, the slow signals lose sensitivity with increasing frequency more quickly than the fast signals, so that by 22.5 Hz the measured phase delays are closer to those of the fast signal (i.e., closer to 0°) (Stockman & Plummer, 2005; Stockman et al., 2005).

Notice that the required phase adjustments fall to close to 0° at a "critical" radiance, which lies between 11.60 and 11.70 $\log_{10}$ quanta s^{-1} deg^{-2} for AS and between 11.65 and 11.75 $\log_{10}$ quanta s^{-1} deg^{-2} for DP. Given that the $+sM-sL$ signals grow relative to the $-sM+sL$ signals as the background radiance increases, there should be a critical background radiance at which the slow signals produced by the 520-nm target all cancel, with the result that the phase delays will then be those of the fast signals and therefore close to 0°—as we find.

Spectral sensitivity

If, as our previous work suggests, the predominant signals change from $-sM$, $+sL$, $+fM$, and $+fL$ below the transition to $+sM$, $-sL$, $+fM$, and $+fL$ above it, there should be clear evidence for both intensity- and frequency-dependent changes in spectral sensitivity across the transition. Moreover, the direction of spectral sensitivity changes should indicate which cone signals destructively or constructively interfere at a particular intensity level.

Figure 4 shows the logarithmic quantal sensitivity ratios for detecting 520 and 650 nm flicker at 2.5, 7.5, 15, and 22.5 Hz for AS (upper panel) and DP (bottom panel). The M- and L-cone sensitivity ratios are shown by the upper and lower horizontal lines, respectively (Stockman & Sharpe, 2000). Two horizontal dashed lines are shown. They represent the spectral sensitivity predictions, if both the M- and the L-cone sensitivities are independently controlled according to Weber's Law, for an additive "luminance" mechanism with L:M cone input weights of 1:1 (upper dashed line) and 2:1 (lower dashed line). If Weber's Law applies, the sensitivity losses for each cone mechanism increase in proportion to the effective background adaptation. Consequently, if the L-cones are 12.9 times more sensitive to the 658-nm field than the M-cones, the 658-nm field will reduce the sensitivity of

the L-cones by 12.9 times more than the sensitivity of the M-cones—with the result that the two adapted cone types become equally sensitive to 658 nm. The Weber limits shown in the figure are calculated by normalizing the L- and M-cone spectral sensitivities at 658 nm and then
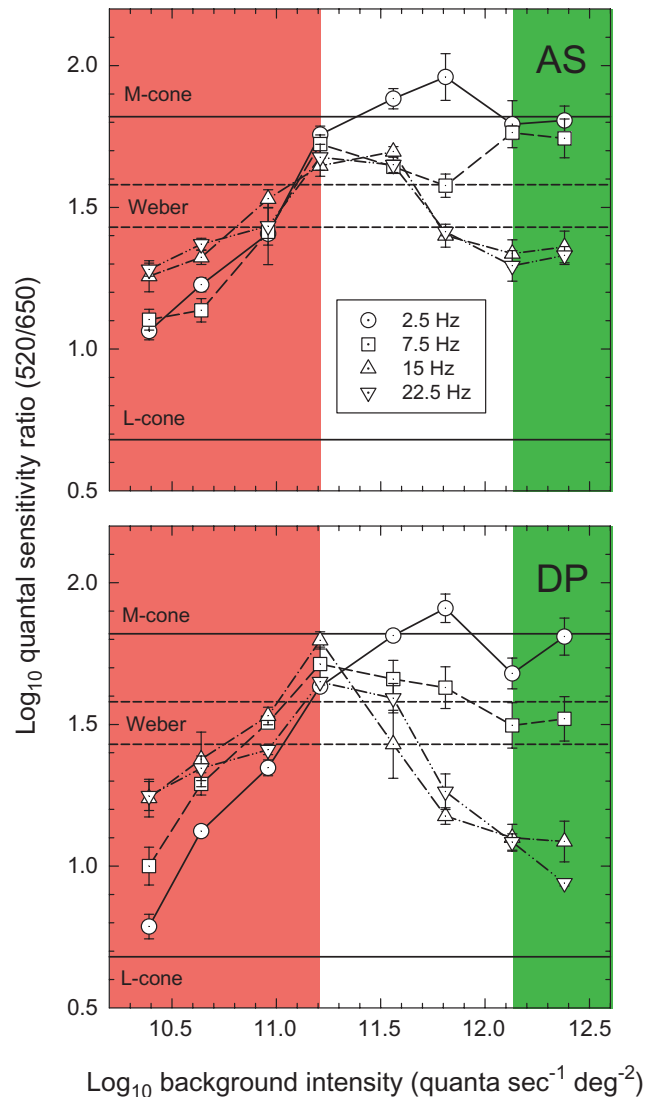

Figure 4. Logarithmic quantal sensitivity ratios for detecting 520- and 650-nm flicker measured as a function of 658-nm background radiance at 2.5 (dotted white circles), 7.5 (dotted white squares), 15 (dotted white triangles), and 22.5 (dotted white inverted triangles) Hz. The pink and green areas correspond to the areas similarly highlighted in Figures 3 and 5. The continuous horizontal lines labeled M- and L-cone are, respectively, the M- and L-cone sensitivity ratios for detecting 520 and 650 nm, and the dashed lines are the Weber's Law predictions. The Weber's Law predictions are calculated by scaling the linear L- and M-cone spectral sensitivities to be equal at the adapting wavelength of 658 nm, and then adding them together in the ratio of 1L:1M (upper dashed lines) or 2L:M (lower dashed lines). All spectral sensitivities are based on the Stockman and Sharpe (2000) cone fundamentals. Upper panel: AS. Lower panel: DP.

linearly combining them with L:M cone weights of 1:1 or 2:1. These weights were chosen to indicate the variation found in the population, which on average favors L but shows considerable individual variability (e.g., Cicerone & Nerger, 1989; De Vries, 1948a; Sharpe, Stockman, Jagla, & Jägle, in press; Stromeyer, Cole, & Kronauer, 1987; Vos & Walraven, 1971; Walraven, 1974). Subject AS is known to have a weight of about 1.7 L:M on a white daylight background (Sharpe et al., in press). If adaptation is limited by Weber's Law, the spectral sensitivity should not cross the appropriate Weber limit for each subject.

At the lowest 658-nm background intensities, the spectral sensitivity ratios for both subjects for detecting 15 and 22.5 Hz flicker are closer to M than those for detecting 2.5 and 7.5 Hz flicker. As the 658-nm background radiance is increased, the selective attenuation of the L-cones by the deep-red field causes the 520/650-nm ratios, as expected, to move towards the Weber limit. Between 11.0 and 11.2 $\log_{10}$ quanta s^{-1} deg^{-2}, however, the Weber's Law predictions are exceeded and the 520/650-nm ratios approach M. Although surprising, this "super-Weber" behavior has been reported at frequencies between 15 and 22.5 Hz several times before (De Vries, 1948b; Eisner & MacLeod, 1981; Stockman, MacLeod, & Vivien, 1993; Stromeyer et al., 1987).

The most remarkable changes in spectral sensitivity occur above 11.3 log quanta s^{-1} deg^{-2}, where the 520/650-nm ratios for the detection of 15- and 22.5-Hz flicker fall precipitously, cross the Weber limit again, and approach L (Stockman, Montag, & MacLeod, 1991). Indeed, the ratio for DP reaches as low as 1 log unit, whereas that for AS reaches about 1.35 log unit. These changes are opposite to the expected effects of chromatic adaptation, which predicts the spectral sensitivities to be close to the Weber limits. The sensitivity ratios for 2.5 Hz, in contrast, remain close to M, whereas those for 7.5 Hz remain roughly between M and the Weber limit. This frequency-dependent difference is important because it shows that the change is not just an overall suppression of the M-cone signal.

The interpretation of the spectral sensitivity data in terms of the model can be simplified by considering separately the effects of signal interactions on the resultant M- and L-cone signals. According to our model, the predominant signals at the lower levels are −sM, +sL, +fM, and +fL. Thus, at low frequencies the M-cone signals cancel and the L-cone signals sum (so causing a spectral sensitivity shift towards L), but at higher frequencies, because of the delay of the slow signals, the M-cone signals constructively interfere and the L-cone signals destructively interfere (so causing a shift towards M). In contrast, the predominant signals at higher levels are +sM, −sL, +fM, and +fL. Thus, at low frequencies the M-cone signals sum and the L-cone signals cancel (so causing a shift towards M), whereas at higher frequencies, again because the

delay of the slow signals, the M-cone signals will destructively interfere and the L-cone signals constructively interfere (so causing a shift towards L). Our data are broadly consistent with these predicted shifts.

At the critical radiance at which the −sM+sL and +sM−sL signals are assumed to cancel, the spectral sensitivity will be that of the fast signals (+fM and +fL). Given that the two fast signals are additive with little phase delay between them, the spectral sensitivity at the critical radiance should be close to the Weber's Law prediction, which is roughly the case for both subjects at 7.5, 15, and 22.5 Hz. At 2.5 Hz, the spectral sensitivity is probably influenced by that of the "true" chromatic channel (which generates a color percept but does not cancel luminance flicker).

Photopigment bleaching becomes significant at the highest field radiances. It has the effect of reducing the cone photopigment optical density and narrowing the cone spectral sensitivity functions (for a discussion, see Stockman & Sharpe, 1999). Consequently, it increases the 520/650-nm sensitivity ratio and reduces the paradoxical shift towards L that we find at the highest levels.

Flicker detection

Figure 5 shows the flicker detection threshold versus radiance (FTVR) curves for AS (top panel) and DP (bottom panel) from which the sensitivity ratios shown in Figure 4 are calculated. The dashed diagonal lines, which correspond to Weber's Law (i.e., a slope of one in double-logarithmic coordinates), are shown for comparison.

Several features of the FTVR functions are noteworthy. The most obvious feature is that the slopes of the 15- and 22.5-Hz curves for detecting 520-nm flicker exceed Weber's Law in the unshaded area of the figure between 11.21 and 12.13 $\log_{10}$ quanta s^{-1} deg^{-2} (having a mean slope of c. 1.1 for AS and 1.3 for DP). A second feature is that the 520-nm FTVR curves fall short of Weber's Law in the pink area below 11.21 $\log_{10}$ quanta s^{-1} deg^{-2}. This shortfall reflects mainly the fact that Weber's Law has not yet been reached by the M-cones on the deep-red field, but it may also be due in part to constructive interference. A third feature is that the 650-nm FTVR curves for both AS and DP roughly follow Weber's Law at all intensities, except perhaps for some slight steepening just before 11.21 $\log_{10}$ quanta s^{-1} deg^{-2}.

According to our model, these FTVR curves, like the spectral sensitivity data, should reflect the effects of destructive and constructive interference between the slow and fast signal components. Those regions within which destructive interference occurs might be expected to have relatively steep slopes (because the signals cancel and reduce sensitivity), whereas those in which constructive interference occurs might be expected to have relatively shallow slopes (because the signals add and increase sensitivity).
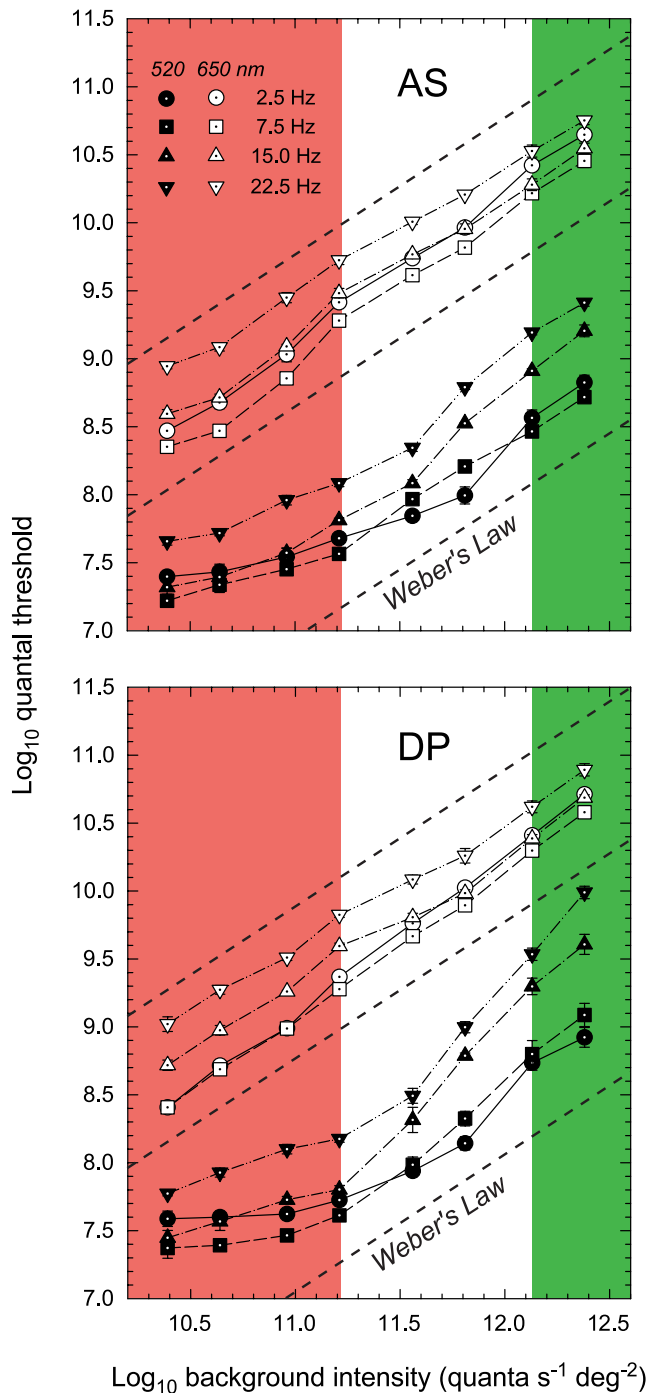
Figure 5. FTVR curves measured at 2.5 (dotted circles), 7.5 (dotted squares), 15 (dotted triangles), and 22.5 (dotted inverted triangles) Hz for 520-nm (black symbols) and 650-nm (white symbols) flicker as a function of the 658-nm background radiance. The shaded areas correspond to the areas similarly shaded in Figures 3 and 4. Upper panel: AS. Lower panel: DP.

We interpret the "super-Weber" behavior between 11.21 and 12.13 $\log_{10}$ quanta s^{-1} deg^{-2} for 15 and 22.5 Hz, 520 nm flicker as being due to a change from constructive interference between the delayed $-sM$ signal and fast $+fM(+fL)$ signals at low levels to destructive interference

between the delayed $+sM$ signal and fast $+fM(+fL)$ signals at higher levels. The slopes for the detection of 2.5 and 7.5 Hz 520 nm are shallower than those for 15 and 22.5 Hz but do not fall below Weber's Law presumably because of cancellation between $-sM$ and $+sM$ signals in the transition region. The 650-nm FTVR curves for DP and AS roughly follow Weber's Law at all frequencies, which is consistent with Weberian adaptation of the fast signals, except for a slight elevation of the curves for AS below 11.21 $\log_{10}$ quanta s^{-1} deg^{-2}. This elevation may reflect an imbalance between the $+sL$ and $-sM$ signals at that level.

Discussion

The results presented here illustrate the large frequency- and intensity-dependent changes that occur as the radiance of a deep-red field is increased from moderate to high levels. We interpret these changes as reflecting changes in the relative strengths of three M-cone signals ($+sM$, $-sM$, and $+fM$) and of three L-cone signals ($+sL$, $-sL$, and $+fL$), all of which we assume contribute to "luminance" (see Figure 6). Below deep-red background radiances of about 11.21 $\log_{10}$ quanta s^{-1} deg^{-2}, the dominant slow signals are $+sL$ and $-sM$ (Stockman & Plummer, 2005), whereas above about 12.13 $\log_{10}$ quanta s^{-1} deg^{-2} they are $-sL$ and $+sM$ (Stockman et al., 2005). The two fast signals ($+fM$ and $+fL$) are consistent with the conventional nonopponent inputs to the luminance channel, whereas the slow signals ($+sL-sM$ or $+sM-sL$) are spectrally opponent inputs. The existence of opponent inputs might be taken as evidence that our flicker cancellation paradigm is influenced not just by the output of the luminance pathway but also by the output of a classical, red-green chromatic pathway. Two properties of
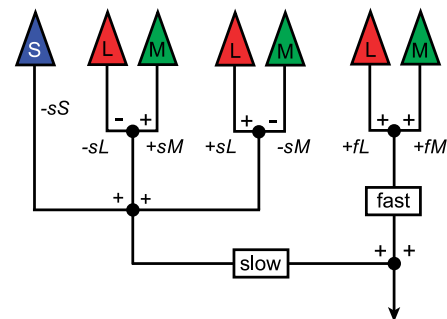

Figure 6. A model of the signals underlying achromatic luminance flicker perception. Slow, spectrally opponent $-sM+sL$ and $+sM-sL$ cone signals are assumed to interact with faster, nonopponent $+fM+fL$ cone signals. The slow, inverted S-cone input is based on earlier work (Lee & Stromeyer, 1989; Stockman, MacLeod, & DePriest, 1987; Stockman, MacLeod, et al., 1991).

the signals involved counter such an interpretation. First, the slow flicker signals produce an achromatic percept that can be flicker photometrically cancelled with luminance flicker; they do not produce a chromatic percept that might be expected of a red-green chromatic signal. Second, the temporal frequency responses of the slow signals extend to moderately high frequencies (Stockman & Plummer, 2005; Stockman et al., 2005), well beyond the temporal frequency response of the psychophysically defined chromatic pathway (see, for example, De Lange, 1958a; Wisowaty, 1981). Further evidence for this model and further discussion can be found in our previous papers (Stockman & Plummer, 2005; Stockman et al., 2005). The idea that there can be a spectrally opponent signal that does not contribute to chromatic perception was also raised by Stromeyer, Kronauer, Ryu, Chaparro, and Eskew (1995) in the context of motion detection. In a later paper, Stromeyer, Chaparro, Tolias, and Kronauer (1997) argued that such signals might be advantageous because they can make isoluminant stimuli visible to the luminance pathway.

The data collected for the main experiments described here were obtained at frequencies of 2.5, 7.5, 15, and 22.5 Hz. At 7.5 Hz and above, good flicker nulls were possible under all conditions, which is consistent with there being little or no chromatic intrusion at those frequencies. In contrast, although 2.5 Hz flicker nulls could be set under nearly all conditions, they were sometimes flicker minima rather than perfect nulls. The 2.5-Hz data, therefore, probably reflect some mixing of luminance and chromatic signals.

The focus of this paper was on the intensity-dependent transition from $+sL-sM$ to $+sM-sL$. Our data are consistent with the transition being caused by a growth in the size of the $+sL-sM$ signal relative to the size of $+sM-sL$ signal as the background radiance is increased, the two signals being equal in amplitude at some "critical" radiance. Because the signals are opposite in polarity, this critical radiance will be marked, not only by the amplitude of the resultant slow signal falling to a minimum, but also by a phase reversal, as we find. We explicitly assume, therefore, that the phase reversal is due to a change in the balance of two underlying mechanisms rather than a change in the polarity of a unitary mechanism. These transitions are not restricted to the 658-nm field: they can also be found on fields of 578, 600, and 633 nm (Stockman & Plummer, personal communication).

We note that our data do not allow us to exclude an alternative hypothesis that the transition reflects the polarity reversals of a population of unitary mechanisms with slightly different reversal intensities. However, the observation (see above) that the slow signals above the transition are slower than those below it suggests that two distinct mechanisms are involved. Moreover, a model in which two pairs of slow inputs partially cancel each other helps to explain why the slow luminance signals are comparatively small under most conditions and why they become perceptually significant only when one or the other is relatively suppressed by chromatic adaptation.

Earlier psychophysical work

The identification of the $-sM$ and $+sM$ inputs and their interactions with the $+fM$ and $+fL$ signals were reported by us in preliminary form (Stockman, Montag, et al., 1991; Stockman & Plummer, 1994). We have since extended our measurements and refined our analyses to produce a more complete model, in which each slow M-cone signal is paired with a spectrally opponent slow L-cone signal (see Figure 6 and Stockman & Plummer, 2005; Stockman et al., 2005). In the interim, some of our work has been replicated, confirming our preliminary conclusions.

Clear psychophysical evidence for slow, inverted inputs to the luminance channel can be found in the earlier phase delay data of Lindsey et al. (1986) and Swanson et al. (1987), although the results were not originally interpreted as such. The $+sM$ and $-sM$ inputs were explicitly identified as a luminance inputs by Stockman et al. (1991) and Stockman and Plummer (1994), respectively. Subsequent to this work, Stromeyer et al. (1997) replicated some of our original experiments and analysis, and it is gratifying that in their meticulous study they were able to identify both M-cone signals.

Stromeyer et al. (1997, 1995) inferred the presence of the spectrally opponent $+sM-sL$ and $+sL-sM$ signals from phase data obtained mainly from motion experiments and also from flicker experiments (see also Stromeyer et al., 2000). Their novel contribution was to observe that $+sM-sL$ signals predominate on shorter wavelength fields. The idea that slow "chromatic" $+sL-sM$ signals oppose faster "luminance" signals on longer wavelength fields was proposed several years earlier by Smith et al. (1992) to account for data obtained from macaque magnocellular (MC)-projecting ganglion cells. In their model, Smith et al. assume that the $+fM+fL$ signals are the center response of the ganglion cell, whereas the chromatically opponent $+sL-sM$ signals are the surround response.

Physiological considerations

Phase characteristics comparable to the ones that we identify psychophysically can be found not only in the responses of some MC ganglion cells (Smith et al., 1992), but also in the responses of some macaque parvocellular (PC) ganglion or LGN cells (Gouras & Zrenner, 1979; Lankheet, Lennie, & Krauskopf, 1998) (although other studies of PC responses show smaller temporal

frequency-dependent effects than we find here; Benardete & Kaplan, 1997; Derrington, Krauskopf, & Lennie, 1984; Lee, Martin, & Valberg, 1989; Lee, Pokorny, Smith, & Kremers, 1994; Smith et al., 1992). Such data point to a retinal source for the signal interactions that we identify psychophysically. We should, however, be cautious about making overly simple connections between retinal physiology and human psychophysics, because any signals found in the retina are likely to be modified by multiple stages before guiding the observer's response in any psychophysical task. Nevertheless, the recent report that PC signals can be identified in the responses of MC cells by Sun and Lee (2004) lends support to the idea that these interactions might be occurring as early as the retina.

A cortical origin for the signal interactions is also a strong possibility. The substantial delay between the slow and fast signals might arise because of differences in the transmission times of parvocellular and magnocellular signals to the cortex, where the two signals might then interact to generate an achromatic flicker signal. Indeed, the parvocellular system is delayed by on average 17 ms relative to the magnocellular system at the level of the LGN (e.g., Schmolesky et al., 1998), although other estimates at the LGN or cortex are lower at about 10 ms (e.g., Maunsell et al., 1999; Maunsell & Gibson, 1992). These delays are comparable to the delays between the slow and fast signals that we find after correction for selective receptoral adaptation (see Figure 7 of Stockman & Plummer, 2005). There is also plenty of evidence for color-luminance interactions in a sizeable fraction of cells in primary cortex (e.g., Conway, 2001; Cottaris & De Valois, 1998; Gouras, 1974; Hubel & Wiesel, 1968; Lennie, Krauskopf, & Sclar, 1990; Vidyasagar, Kulikowski, Lipnicki, & Dreher, 2002). In a recent, carefully controlled study of cone inputs to macaque V1, Johnson, Hawken, and Shapley (2004) classified 34% of cells as color-luminance cells, 10% as color-preferring cells, and 56% as luminance-preferring cells. Yet another possible route for the slow color signals to interact with flicker (or motion) signals is suggested by the recent finding of a direct geniculate input from mostly koniocellular LGN neurons to MT (Sincich, Park, Wohlgemuth, & Horton, 2004).

Wherever these signal interactions originate, their phase and amplitude characteristics are distinctive enough that they should be unmistakable in physiological recordings made with the appropriate stimuli—assuming, that is, that the interaction can be measured in a single neurons (rather than in a network).

Are very high intensity red fields effectively green after the photoreceptors?

The slow, spectrally opponent $+sM-sL$ signals that prevail under conditions of very intense long-wavelength adaptation also prevail on adapting fields of wavelengths shorter than c. 570 nm (Stockman & Plummer, personal communication; Stromeyer et al., 1997). But why should an intense long-wavelength field and a short or middle-wavelength field both reveal the same postreceptoral signals? Intensity-dependent changes in color appearance, which are known collectively as the Bezold–Brücke effect, are well documented. Purdy (1931), in a fairly extensive study, reported that the appearance of long-wavelength lights shifted from red towards yellow with increasing radiance, but no further; there being an invariant wavelength at about 575 at which no change in apparent color with radiance was found. This observation is consistent with first-order kinetics, which predicts that the asymptotic sensitivity of a cone at high bleaching levels should be limited by Weber's Law. Thus, although intense long-wavelength bleaching lights would be expected to become postreceptorally neutral at high intensities (because the two cone types become equally sensitive to the background; see also above), they would not be expected to have an effect comparable to a short- or middle-wavelength light.

Purdy's observations, however, were made on only moderate to high intensity long-wavelength fields. At very high intensities, the apparent color of a long-wavelength field gradually changes from red to yellow and finally to green, which remains the "steady-state" appearance (Auerbach & Wald, 1955; Cornsweet, Fowler, Rabedeau, Whalen, & Williams, 1958). Indeed, we also observe that very intense long-wavelength backgrounds (above the transition from $+sL-sM$ to $-sL+sM$) obtain a green tinge under steady-state conditions. Interestingly, Cornsweet (1962) later contradicted his earlier conclusions (which were inconsistent with a first-order model of kinetics) and reported that the green appearance eventually faded back to yellow. We do not observe such a change on our brightest 658-nm fields.

For long-wavelength fields to become effectively green after the photoreceptors, the additional loss of sensitivity in the L-cones to the background caused by bleaching has to exceed Weber's Law before the loss of sensitivity in the M-cones reaches the same level. There is, in fact, good evidence that the L-cone loss will exceed that of the M-cone, because, although first-order bleaching kinetics is a useful simplification, the kinetics are, nonlinear. Several studies now concur that bleaching actually falls below the first-order prediction at low bleaching levels and above it at high (e.g., Burns & Elsner, 1985, 1989; Mahroo & Lamb, 2004; Reeves, Wu, & Schirillo, 1998; Smith, Pokorny, & van Norren, 1983). See, in particular, Figure 11B and Equation A10 of Mahroo & Lamb (2004); and for a general discussion, see Lamb & Pugh (2004). The additional loss of L-cone sensitivity to the background caused by nonlinear kinetics at high bleaching levels could be sufficient to make a high intensity long-wavelength bleaching field act postreceptorally more like a short- or middle-wavelength field.

We speculate that the critical long-wavelength background radiance is equivalent to a physiologically "neutral"

background in the sense that the M- and L-cone signals it generates are balanced postreceptorally. On such a background, we assume that the slow signals are minimized by destructive interference (see Stockman & Plummer, 2005).

Suppression of the fast M-cone signal (+fM) by long-wavelength fields

We assume that the weights of the +sM versus −sL and +sL versus −sM inputs are balanced so that no slow signal is found under equichromatic conditions, when the target and background are of the same wavelength. To the extent that this assumption is true, the differences between m for the M- and for the L-cones (see Table 1) must therefore reflect differences between the amplitudes of the two fast signals (i.e., +fL > +fM, by the ratio of m for the M-cones divided by m for the L-cones). A stronger +fL than +fM cone signal is expected in most subjects, simply because the L-cone contribution to luminance is usually larger than the M-cone contribution (e.g., De Vries, 1948a; Smith & Pokorny, 1975; Stromeyer et al., 1985; Vos & Walraven, 1971; Walraven, 1974; Sharpe et al., in press), an asymmetry that is also found for our subjects, AS and DP. The asymmetries that we find, however, are too large to be due solely to different L- and M-cone contributions to luminance. We must suppose, therefore, that the intense long-wavelength field causes an additional and selective suppression of the +fM signal (or M-cone luminance input).

Another aspect of our data is also consistent with an additional suppression of the +fM signal by the long-wavelength field. At Level 4, the flicker spectral sensitivity at 22.5 Hz is as close to the L-cone spectral sensitivity as it is at 15 Hz (see also Figure 3 of Stockman et al., 2005). Given that the slow M-cone signals (+sM) and fast M- and L-cone signals (+fM and +fL) are only about 90° (DP) or 120° (AS) apart at 22.5 Hz (according to the model fits), the shift to an L-cone spectral sensitivity at this frequency cannot be entirely due to destructive interference. Such a shift towards L is also consistent with a selective suppression of the +fM signals under conditions of long-wavelength adaptation, as are the very high slow/fast signal ratio (m) values for the M-cones but not for L-cones (see Table 1). This suppression seems to be confined to the fast M-cone signals because the spectral sensitivities at 2.5 Hz and 7.5 Hz are not similarly shifted towards L even at the highest background radiance.

Our evidence for a relative suppression of the +fM signal on deep-red fields might seem at odds with the conclusions of others, based on 15- and 22.5-Hz flicker spectral sensitivity data, that it is the +fL signal (or L-cone luminance input) that is suppressed (Eisner & MacLeod, 1981; Stromeyer et al., 1997; Stromeyer et al., 1987). However, our evidence and model suggest that any "suppres-

sion" of L is restricted to moderate long-wavelength intensities (being largest near 11.21 $\log_{10}$ quanta s^{-1} deg^{-2}) and is due to a large extent to destructive interference between the slow and fast cone signals rather than to suppression. The suppression that we find under conditions of long-wavelength adaptation is mainly a suppression of the +fM signals (see the m values in Table 1).

Stiles π mechanisms

The changes in the slopes of the FTVR curves shown in Figure 5 are reminiscent of the changes in the slopes of threshold-versus-radiance (TVR) curves identified by Stiles as a transition from π_4 to π_4' or from π_5 to π_5' (Stiles, 1953). The transitions between low (π_4) and high (π_4') intensity forms of predominantly M-cone mechanisms, or between low (π_5) and high (π_5') intensity forms of predominantly L-cone mechanisms, were the subject of some experimental interest in the early 1980s (e.g., Kirk, 1985; Reeves, 1982; Sigel & Brousseau, 1982; Sigel & Pugh, 1980; Wandell & Pugh, 1980). We suggest that the transition from π_4 to π_4' found on deep-red 667-nm fields reflects the same underlying change from −sM+sL to +sM−sL that we report here.

Conclusions

Under long-wavelength adaptation, fast nonopponent signals (+fM+fL) and slow spectrally opponent signals (+sM−sL and −sM+sL) contribute to achromatic luminance flicker perception. These signals constructively and destructively interfere to produce characteristic, frequency-dependent changes in spectral sensitivity and phase delay data without producing visible color variation. The two spectrally opponent signals seem to coexist at some levels, but their relative contributions to luminance change from a predominance of −sM+sL at low long-wavelength adaptation levels to a predominance of +sM−sL at high levels.

Acknowledgments

Commercial relationships: none.
Corresponding author: Andrew Stockman.
Email: a.stockman@ucl.ac.uk.
Address: Institute of Ophthalmology, University College London, 11–43 Bath Street, London EC1V 9EL, UK.

References

Auerbach, E., & Wald, G. (1955). The participation of different types of cones in human light and dark adaptation. *American Journal of Ophthalmology, 39,* 24–40. [PubMed]

Benardete, E. A., & Kaplan, E. (1997). The receptive field of primate P retinal ganglion cell: I. Linear dynamics. *Visual Neuroscience, 14,* 169–185. [PubMed]

Boynton, R. M. (1979). *Human color vision.* New York: Holt, Rinehart and Winston.

Burns, S. A., & Elsner, A. E. (1985). Color matching at high luminances: The color-match-area effect and photopigment bleaching. *Journal of the Optical Society of America A, 2,* 698–704. [PubMed]

Burns, S. A., & Elsner, A. E. (1989). Localizing color vision deficiencies in eye disease. *Documenta Opthalmologica Proceedings Series,* IX (pp. 167–180). Dordrecht: Kluwer Academic Publishers.

Chaparro, A., Stromeyer, C. F., III, Chen, G., & Kronauer, R. E. (1995). Human cones appear to adapt at low light levels: Measurements on the red-green detection mechanism. *Vision Research, 35,* 3103–3118. [PubMed]

Cicerone, C. M., & Nerger, J. L. (1989). The relative numbers of long-wavelength-sensitive to middle-wavelength-sensitive cones in the human fovea centralis. *Vision Research, 29,* 115–128. [PubMed]

Conway, B. R. (2001). Spatial structure of cone inputs to color cells in alert macaque primary visual cortex (V-1). *Journal of Neuroscience, 21,* 2768–2783. [PubMed]

Cornsweet, T. N. (1962). Changes in the appearance of stimuli of very high luminance. *Psychological Review, 69,* 257–273. [PubMed]

Cornsweet, T. N., Fowler, H., Rabedeau, R. G., Whalen, R. E., & Williams, D. R. (1958). Changes in the perceived color of very bright stimuli. *Science, 128,* 898–899. [PubMed]

Cottaris, N. P., & De Valois, R. L. (1998). Temporal dynamics of chromatic tuning in macaque primary visual cortex. *Nature, 395,* 896–900. [PubMed]

Cushman, W. B., & Levinson, J. Z. (1983). Phase shift in red and green counter-phase flicker at high frequencies. *Journal of the Optical Society of America, 73,* 1557–1561. [PubMed]

De Lange, H. (1958a). Research into the dynamic nature of the human fovea-cortex systems with intermittent and modulated light: I. Attenuation characteristics with white and colored light. *Journal of the Optical Society of America, 48,* 777–784.

De Lange, H. (1958b). Research into the dynamic nature of the human fovea-cortex systems with intermittent and modulated light: II. Phase shift in brightness and delay in color perception. *Journal of the Optical Society of America, 48,* 784–789.

De Vries, H. (1948a). The heredity of the relative numbers of red and green receptors in the human eye. *Genetica, 24,* 199–212.

De Vries, H. (1948b). The luminosity curve of the eye as determined by measurements with the flicker photometer. *Physica, 14,* 319–348.

Derrington, A. M., Krauskopf, J., & Lennie, P. (1984). Chromatic mechanisms in lateral geniculate nucleus of macaque. *Journal of Physiology, 357,* 241–265. [PubMed]

Eisner, A., & MacLeod, D. I. A. (1980). Blue sensitive cones do not contribute to luminance. *Journal of the Optical Society of America, 70,* 121–123. [PubMed]

Eisner, A., & MacLeod, D. I. A. (1981). Flicker photometric study of chromatic adaptation: Selective suppression of cone inputs by colored backgrounds. *Journal of the Optical Society of America, 71,* 705–718. [PubMed]

Eskew, R. T., McLellan, J. S., & Giulianini, F. (1999). Chromatic detection and discrimination. In K. Gegenfurtner & L. T. Sharpe (Eds.), *Color vision: From genes to perception.* Cambridge: Cambridge University Press.

Gouras, P. (1974). Opponent-colour cells in different layers of foveal striate cortex. *Journal of Physiology, 238,* 583–602. [PubMed]

Gouras, P., & Zrenner, E. (1979). Enhancement of luminance flicker by color-opponent mechanisms. *Science, 205,* 587–589. [PubMed]

Guth, S. L., Alexander, J. V., Chumbly, J. I., Gillman, C. B., & Patterson, M. M. (1968). Factors affecting luminance additivity at threshold. *Vision Research, 8,* 913–928. [PubMed]

Hubel, D. H., & Wiesel, T. N. (1968). Receptive fields and functional architecture of monkey striate cortex. *Journal of Physiology, 195,* 215–243. [PubMed]

Johnson, E. N., Hawken, M. J., & Shapley, R. (2004). Cone inputs in macaque primary visual cortex. *Journal of Neurophysiology, 91,* 2501–2514. [PubMed]

Kirk, D. B. (1985). The putative π_4 mechanism: Failure of shape invariance and field additivity. *Investigative Ophthalmology and Visual Science, 26*(Suppl.), 184.

Lamb, T. D., & Pugh, E. N., Jr. (2004). Dark adaptation and the retinoid cycle of vision. *Progress in Retinal and Eye Research, 23,* 307–380. [PubMed]

Lankheet, M. J. M., Lennie, P., & Krauskopf, J. (1998). Temporal–chromatic interactions in LGN P-cells. *Visual Neuroscience, 15,* 47–54. [PubMed]

Lee, B. B., Martin, P. R., & Valberg, A. (1989). Sensitivity of macaque retinal ganglion cells to chromatic and luminance flicker. *Journal of Physiology, 414,* 223–243. [PubMed]

Lee, B. B., Pokorny, J., Smith, V. C., & Kremers, J. (1994). Responses to pulses and sinusoids in macaque ganglion cells. *Vision Research, 34,* 3081–3096. [PubMed]

Lee, J., & Stromeyer, C. F., III. (1989). Contribution of human short-wave cones to luminance and motion detection. *Journal of Physiology, 413,* 563–593. [PubMed]

Lennie, P., Krauskopf, J., & Sclar, G. (1990). Chromatic mechanisms in striate cortex of macaque. *Journal of Neuroscience, 10,* 649–669. [PubMed]

Lindsey, D. T., Pokorny, J., & Smith, V. C. (1986). Phase-dependent sensitivity to heterochromatic flicker. *Journal of the Optical Society of America A, 3,* 921–927. [PubMed]

Luther, R. (1927). Aus dem Gebiet der Farbreizmetrik. *Zeitschrift fürTtechnische Physik, 8,* 540–558.

Mahroo, O. A. R., & Lamb, T. D. (2004). Recovery of the human photopic electroretinogram after bleaching exposures: Estimation of pigment regeneration kinetics. *Journal of Physiology, 554,* 417–437. [PubMed]

Maunsell, J. H., Ghose, G. M., Assad, J. A., McAdams, C. J., Boudreau, C. E., & Noerager, B. D. (1999). Visual response latencies of magnocellular and parvocellular LGN neurons in macaque monkeys. *Visual Neuroscience, 16,* 1–14. [PubMed]

Maunsell, J. H., & Gibson, J. R. (1992). Visual response latencies in striate cortex of the macaque monkey. *Journal of Neurophysiology, 68,* 1332–1344. [PubMed]

Purdy, D. M. (1931). Spectral hue as a function of intensity. *American Journal of Psychology, 63,* 541–559.

Reeves, A. (1982). π_4: Adaptation of one class of cone. *Journal of the Optical Society of America, 72,* 1437–1438.

Reeves, A., Wu, S., & Schirillo, J. (1998). The effect of photon noise on the detection of white flashes. *Vision Research, 38,* 691–703. [PubMed]

Schmolesky, M. T., Wang, Y., Hanes, D. P., Thompson, K. G., Leutgeb, S., Schall, J. D., et al. (1998). Signal timing across the macaque visual system. *Journal of Neurophysiology, 79,* 3272–3278. [PubMed]

Schrödinger, E. (1925). Über das Verhältnis der Vierfarben zur Dreifarbentheorie. *Sitzungberichte. Abt. 2a, Mathematik, Astronomie, Physik, Meteorologie und Mechanik. Akademie der Wissenschaften in Wien, Mathematisch-Naturwissenschaftliche Klasse, 134,* 471.

Sharpe, L. T., Stockman, A., Jagla, W., & Jägle, H. (in press). A luminous efficiency function, $V^*(\lambda)$, for daylight adaptation. *Journal of Vision.*

Sigel, C., & Brousseau, L. (1982). π_4: Adaptation of more than one class of cone. *Journal of the Optical Society of America, 72,* 237–246. [PubMed]

Sigel, C., & Pugh, E. N., Jr. (1980). Stiles's π_5 color mechanism: Tests of field displacements and field additivity properties. *Journal of the Optical Society of America, 70,* 71–81. [PubMed]

Sincich, L. C., Park, K. F., Wohlgemuth, M. J., & Horton, J. C. (2004). Bypassing V1: A direct geniculate input to area MT. *Nature Neuroscience, 7,* 1123–1128. [PubMed]

Smith, V. C., Lee, B. B., Pokorny, J., Martin, P. R., & Valberg, A. (1992). Responses of macaque ganglion cells to the relative phase of heterochromatically modulated lights. *Journal of Physiology, 458,* 191–221. [PubMed]

Smith, V. C., & Pokorny, J. (1975). Spectral sensitivity of the foveal cone photopigments between 400 and 500 nm. *Vision Research, 15,* 161–171. [PubMed]

Smith, V. C., Pokorny, J., & van Norren, D. (1983). Densitometric measurement of human cone photopigment kinetics. *Vision Research, 23,* 517–524. [PubMed]

Stiles, W. S. (1953). Further studies of visual mechanisms by the two-colour threshold technique. *Coloquio Sobre Problemas Opticos de la Vision, 1,* 65–103.

Stockman, A., MacLeod, D. I. A., & DePriest, D. D. (1987). An inverted S-cone input to the luminance channel: Evidence for two processes in S-cone flicker detection. *Investigative Ophthalmology and Visual Science, 28*(Suppl.), 92.

Stockman, A., MacLeod, D. I. A., & DePriest, D. D. (1991). The temporal properties of the human short-wave photoreceptors and their associated pathways. *Vision Research, 31,* 189–208. [PubMed]

Stockman, A., MacLeod, D. I. A., & Vivien, J. A. (1993). Isolation of the middle- and long-wavelength sensitive cones in normal trichromats. *Journal of the Optical Society of America A, 10,* 2471–2490. [PubMed]

Stockman, A., Montag, E. D., & MacLeod, D. I. A. (1991). Large changes in phase delay on intense bleaching backgrounds. *Investigative Ophthalmology and Visual Science, 32*(Suppl.), 841.

Stockman, A., & Plummer, D. J. (1994). The luminance channel can be opponent? *Investigative Ophthalmology and Visual Science, 35*(Suppl.), 1572.

Stockman, A., & Plummer, D. J. (2005). Spectrally opponent inputs to the human luminance pathway: Slow +L and −M cone inputs revealed by low to moderate

long-wavelength adaptation. *Journal of Physiology, 566,* 77–91. [PubMed]

Stockman, A., & Plummer, D. J. (in preparation). *Slow, spectrally-opponent inputs to the human luminance pathway.*

Stockman, A., Plummer, D. J., & Montag, E. D. (2005). Spectrally-opponent inputs to the human luminance pathway: Slow +M and −L cone inputs revealed by intense long-wavelength adaptation. *Journal of Physiology, 566,* 61–76. [PubMed]

Stockman, A., & Sharpe, L. T. (1999). Cone spectral sensitivities and color matching. In K. Gegenfurtner & L. T. Sharpe (Eds.), *Color vision: From genes to perception* (pp. 53–87). Cambridge: Cambridge University Press.

Stockman, A., & Sharpe, L. T. (2000). Spectral sensitivities of the middle- and long-wavelength sensitive cones derived from measurements in observers of known genotype. *Vision Research, 40,* 1711–1737. [PubMed]

Stromeyer, C. F., III, Chaparro, A., Tolias, A. S., & Kronauer, R. E. (1997). Colour adaptation modifies the long-wave versus middle-wave cone weights and temporal phases in human luminance (but not red-green) mechanism. *Journal of Physiology, 499,* 227–254. [PubMed]

Stromeyer, C. F., III, Cole, G. R., & Kronauer, R. E. (1985). Second-site adaptation in the red-green chromatic pathways. *Vision Research, 25,* 219–237. [PubMed]

Stromeyer, C. F., III, Cole, G. R., & Kronauer, R. E. (1987). Chromatic suppression of cone inputs to the luminance flicker mechanisms. *Vision Research, 27,* 1113–1137. [PubMed]

Stromeyer, C. F., III, Gowdy, P. D., Chaparro, A., Kladakis, S., Willen, J. D., & Kronauer, R. E. (2000). Colour adaptation modifies the temporal properties of the long- and middle-wave cone signals in the human luminance mechanism. *Journal of Physiology, 526,* 177–194. [PubMed]

Stromeyer, C. F., III, Kronauer, R. E., Ryu, A., Chaparro, A., & Eskew, R. T. (1995). Contributions of human long-wave and middle-wave cones to motion detection. *Journal of Physiology, 485,* 221–243. [PubMed]

Sun, H., & Lee, B. B. (2004). The origin of the chromatic response of magnocellular ganglion cells [Abstract]. *Journal of Vision, 4*(11), 18a, http://journalofvision.org/4/11/18/, doi:10.1167/4.11.18.

Swanson, W. H., Pokorny, J., & Smith, V. C. (1987). Effects of temporal frequency on phase-dependent sensitivity to heterochromatic flicker. *Journal of the Optical Society of America A, 4,* 2266–2273. [PubMed]

Vidyasagar, T. R., Kulikowski, J. J., Lipnicki, D. M., & Dreher, B. (2002). Convergence of parvocellular and magnocellular information channels in the primary visual cortex of the macaque. *European Journal of Neuroscience, 16,* 945–956. [PubMed]

Vos, J. J., & Walraven, P. L. (1971). On the derivation of the foveal receptor primaries. *Vision Research, 11,* 799–818. [PubMed]

Walls, G. L. (1955). A branched-pathway schema for the color-vision system and some of the evidence for it. *American Journal of Ophthalmology, 39,* 8–23. [PubMed]

Walraven, P. L. (1974). A closer look at the tritanopic confusion point. *Vision Research, 14,* 1339–1343. [PubMed]

Walraven, P. L., & Leebeek, H. J. (1964). Phase shift of sinusoidally alternating colored stimuli. *Journal of the Optical society of America, 54,* 78–82. [PubMed]

Wandell, B. A., & Pugh, E. N., Jr. (1980). Detection of long-duration incremental flashes by a chromatically coded pathway. *Vision Research, 20,* 625–635. [PubMed]

Wisowaty, J. J. (1981). Estimates for the temporal response characteristics of chromatic pathways. *Journal of the Optical Society of America, 71,* 970–977. [PubMed]